ISSN (Print) : 2320 – 3765
ISSN (Online): 2278 – 8875

International Journal of Advanced Research in Electrical, Electronics and Instrumentation Engineering

(An ISO 3297: 2007 Certified Organization)

Vol. 4, Issue 3, March 2015

A High Step-Up DC–DC Converter for Photovoltaic Applications

Premkumar S[1*], Ramu.G[2], Gunasekaran.S[3], Baskar.D[4]

Assistant Professor, Department of Electrical and Electronics Engineering, Bharath University, Chennai, Tamilnadu, India. [1*,2,3,4],

ABSTRACT: Photovoltaic (PV) power-generation systems are becoming increasingly important and prevalent in distribution generation systems. The dc–dc converter requires large step-up conversion from the panel's low voltage to the voltage level of the application.A coupled inductor integrated with boost converter is used in the system. The proposed converter has several features: The connection of the two pairs of inductors, capacitor, and diode gives a large step-up voltage-conversion ratio; the leakage-inductor energy of the coupled inductor can be recycled, thus increasing the efficiency and restraining the voltage stress across the active switch; and the floating active switch efficiently isolates the PV panel energy during non-operating conditions, which enhances safety. In this paper detailed operating principles and steady-state analyses of continuous modes are described. A 15 V input voltage, 200 V output voltage, and 200 W output power prototype circuit of the proposed converter has been simulated.

KEYWORDS: PV cells, Boost converter, coupled inductor, high step-up voltage gain, and single switch.

I. INTRODUCTION

IN RECENT years, growing concerns for the environment have led to increased interest in natural energy sources. A centralized PV array is a serial connection of numerous panels to obtain higher dc-link voltage for main electricity through a dc–ac inverter [1], [30].Unfortunately, once there is a partial shadow on some panels, the system's energy yield becomes significantly reduced [2]. An ac module is a microinverter configured on the rear bezel of a PV panel [1]–[3]; this alternative solution not only immunizes against the yield loss by shadow effect, but also provides flexible installation options in accordance with the user's budget [4]. Many prior research works have proposed a single-stage dc–ac inverter with fewer components to fit the dimensions of the bezel of the ac module, but their efficiency levels are lower than those of conventional PV inverters.

The power capacity range of a single PV panel is about 100 W to 300 W, and the maximum power point (MPP) voltage range is from 15 V to 40 V,which will be the input voltage of the ac module; in cases with lower input voltage, it is difficult for the ac module to reach high efficiency [3]. However, employing a high step-up dc–dc converter in the front of the inverter improves power-conversion efficiency and provides a stable dc link to the inverter. When installing the PV generation system during daylight, for safety reasons, the ac module outputs zero voltage [4], [5].There are two major concerns related to the efficiency of a high step-up dc–dc converter: large input current and high output voltage. The large input current results from low input voltage; therefore, low-voltage-rated devices with low $R_{DS\ on}$ are necessary in order to reduce the conduction loss.

Previous research on various converters for high step-up applications has included analyses of the switched-inductor and switched-capacitor types [6], [7]; transformer less switched-capacitor type [8], [9], [29];the voltage-lift type [12]; the capacitor-diode voltage multiplier[13]; and the boost type integrated with a coupled inductor [10], [11], these converters by increasing turns ratio of coupled inductor obtain higher voltage gain than conventional boost converter. Some converters successfully combined boost and flyback converters, since various converter combinations are developed to carry out high step-up voltage gain by using the coupled-inductor technique [14]–[19], [27], [28]. The efficiency and voltage gain of the dc–dc boost converter are constrained by either the parasitic effect of the power switches or the reverse recovery issue of the diodes. In addition, the equivalent series resistance (ESR) of the capacitor and the parasitic resistances of the inductor also affect overall efficiency. Use of active clamp technique not only recycles the leakage inductor's energy but also constrains the voltage stress across the active switch, however the trade

ISSN (Print) : 2320 – 3765
ISSN (Online): 2278 – 8875

International Journal of Advanced Research in Electrical, Electronics and Instrumentation Engineering

(An ISO 3297: 2007 Certified Organization)

Vol. 4, Issue 3, March 2015

off is higher cost and complex control circuit [25],[26]. By combining active snubber, auxiliary resonant circuit, synchronous rectifiers, or switched- capacitor-based resonant circuits and so on, these techniques made active switch into zero voltage switching (ZVS) or zero current switching (ZCS) operation and improved converter efficiency [20]–[24]. However when the leakage-inductor energy from the coupled inductor can be recycled, the voltage stress on the active switch is reduced, which means the coupled inductor employed in combination with the voltage-multiplier or voltage-lift technique successfully accomplishes the goal of higher voltage gain [6]–[13].The Fig.1 shows the basic block diagram of proposed system.

The proposed converter, shown in Fig.2, is comprised of a coupled inductor T1 with the floating active switch S1. The primary winding N1

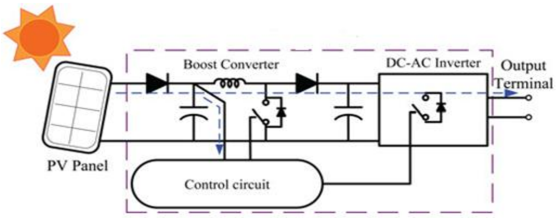

Fig.1 Block diagram of proposed system

of a coupled inductor T1 is similar to the input inductor of the boost converter, and capacitor C1 and diode D1 receive leakage inductor energy from N1. The secondary winding N2 of coupled inductor T1 is connected with another pair of capacitors C2 and diode D2, which are in series with N1 in order to further enlarge the boost voltage. The rectifier diode D3 connects to its output capacitor C3.

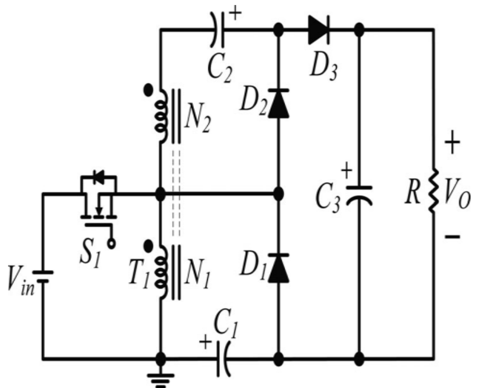

Fig.2. Circuit configuration of Boost converter with coupled inductor.

During boost operation, when switches $S_1$is turned ON, the primary and secondary windings of the coupled inductor are operated in series-discharge to achieve high step-up voltage gain. The operating principles and steady-state analysis of the proposed converter are presented in the following sections.[21-24]

II. OPERATING PRINCIPLES OF THE PROPOSED CONVERTER

The simplified circuit model of the proposed converter is shown in Fig. 3. The coupled inductor T_1 is represented as a magnetizing inductor L_m, primary and secondary leakage inductors $L_{k\,1}$ and $L_{k\,2}$, and an ideal transformer. In order to simplify the circuit analysis of the proposed converter, the following assumptions are made.[26-27]

1) All components are ideal, except for the leakage inductance of coupled inductor T_1, which is being taken under consideration. The on-state resistance $R_{DS(ON)}$ and all parasitic capacitances of the main switch S_1 are neglected, as are the forward voltage drops of diodes D_1~ D_3 .[28-30]

ISSN (Print) : 2320 – 3765
ISSN (Online): 2278 – 8875

International Journal of Advanced Research in Electrical, Electronics and Instrumentation Engineering

(An ISO 3297: 2007 Certified Organization)

Vol. 4, Issue 3, March 2015

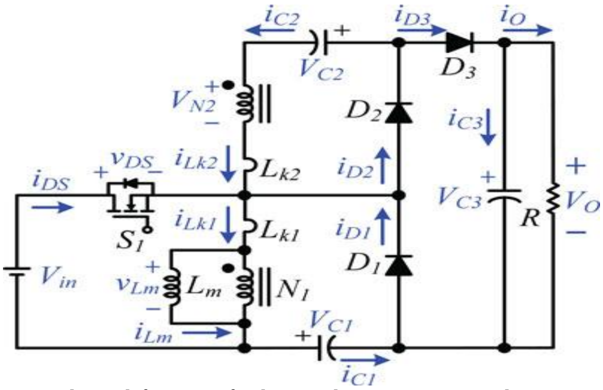

Fig.3.Polarity definitions of voltage and current in proposed converter.

2) The capacitors C_1~C_3 are sufficiently large that the voltages across them are considered to be constant.[14-17]
3) The ESR of capacitors C_1~C_3 and the parasitic resistance of coupled inductor T_1 are neglected.
4) The turns ratio n of the coupled inductor T_1 windings is equal to N_2 / N_1.
The operating principle of continuous conduction mode (CCM) is presented in detail. The current waveforms of major components are given in Fig. 5. There are five operating modes in a switching period. The operating modes are described as follows.[18-20]

Continuous conduction mode (CCM) operation

Mode 1 [t_0, t_1]

In this transition interval, the magnetizing inductor L_m continuously charges capacitor C_2 through T_1 when S_1 is turned ON. The current flow path is shown in Fig. 4.(a) switch S_1 and diode D_2 is conducting. The current I_{Lm} is decreasing because source voltage V_{in} crosses magnetizing inductor L_m and primary leakage inductor L_{k1} magnetizing inductor L_m is still transferring its energy through coupled inductor T_1 to charge switched capacitor C_2 , but the energy is decreasing the charging current i_{D2} and i_{C2} are decreasing. The secondary leakage inductor current i_{LK2} is declining as equal to i_{Lm} / n. Once the increasing i_{Lk1} equals decreasing i_{Lm} at $t = t_1$, this mode ends.[24-25]

Mode 2 [t_1, t_2]

During this interval, source energy V_{in} is series connected with N_2, C_1, and C2 to charge output capacitor C_3 and load R; meanwhile magnetizing inductor L_m is also receiving energy from V_{in}. The current flow path is shown in Fig.4(b), where switch S_1 remains ON and only diode D_3 is conducting. The i_{Lm}, i_{Lk1},and i_{D3} are increasing because the V_{in} is crossing L_{k1} , L_m, and primary winding N_1; L_m and L_{k1} are storing energy

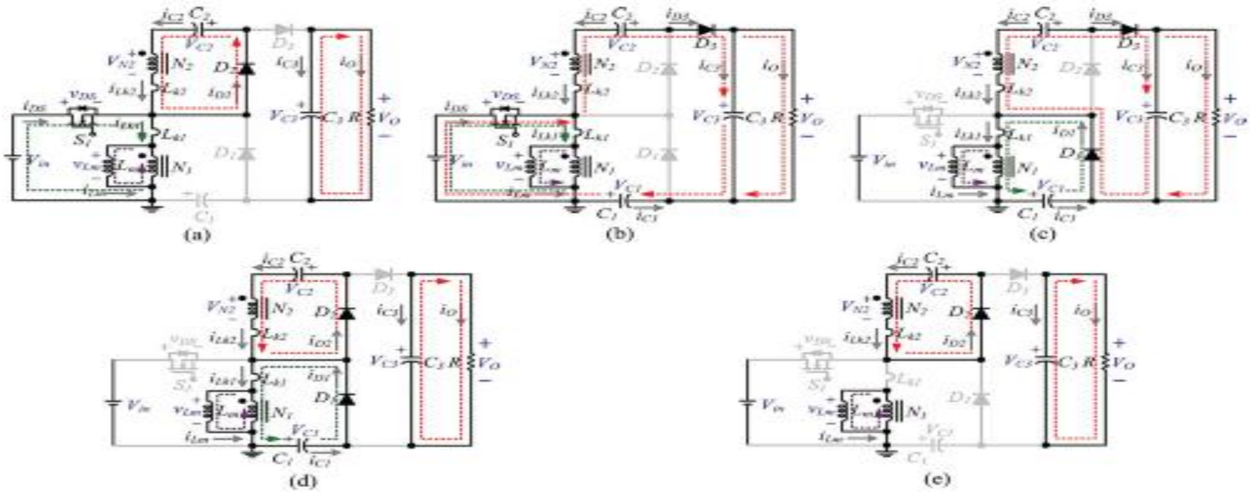

Fig 4 Current flow path of five operating modes during one switching period at CCM operation. (a) Mode I: t0~ t1. (b) Mode II: t_1~t2 (c) Mode III: : t_2~t3 (d)Mode IV: t3~ t4. (e) Mode V: t4~ t5.

ISSN (Print) : 2320 – 3765
ISSN (Online): 2278 – 8875

International Journal of Advanced Research in Electrical, Electronics and Instrumentation Engineering

(An ISO 3297: 2007 Certified Organization)

Vol. 4, Issue 3, March 2015

from V_{in} meanwhile Vin is also serially connected with secondary winding N_2 of coupled inductor T_1, capacitors C_1 , and C_2 , and then discharges their energy to capacitor C_3 and load R. The i_{in}, i_{D3} and discharging current $|i_{C1}|$ and $|i_{C2}|$ are increasing. This mode ends when switch S_1 is turned OFF at $t = t_2$.

Mode 3 [t_2 , t_3]

During this transition interval, secondary leakage inductor L_{k2} keeps charging C_3 when switch S_1 is OFF. The current flow path is shown in Fig.4(c), where only diode D_1 and D_3 are conducting. The energy stored in leakage inductor L_{k1} flows through diode D_1 to charge capacitor C_1 instantly when S_1 is OFF. Meanwhile, the energy of secondary leakage inductor L_{k2} is series connected with C_2 to charge output capacitor C_3 and the load. Because leakage inductance L_{k1} andL_{K2} are far smaller than L_m, i_{Lk2} rapidly decreases, but i_{Lm} is increasing because magnetizing inductor Lm is receiving energy from L_{k1}. Current i_{Lk2} decreases until it reaches zero; this mode ends at $t = t_3$.

Mode 4 [t_3 , t_4]

During this transition interval, the energy stored in magnetizing inductor L_m is released to C_1 and C_2 simultaneously.[31-33] The current flow path is shown in Fig.4(d). Only diodes D_1 and D_2 are conducting. Currents i_{Lk1} and i_{D1} are continually decreased because the leakage energy still flowing through diodeD_1 keeps charging capacitor C_1. The L_m is delivering its energy through T_1 and D_2 to charge capacitor C_2.The energy stored in capacitor C_3 is constantly discharged to the load R. These energy transfers result in decreases in i_{Lk1} and i_{Lm} but increases in i_{Lk2} .This mode ends when current i_{Lk1} is zero, at $t = t_4$.

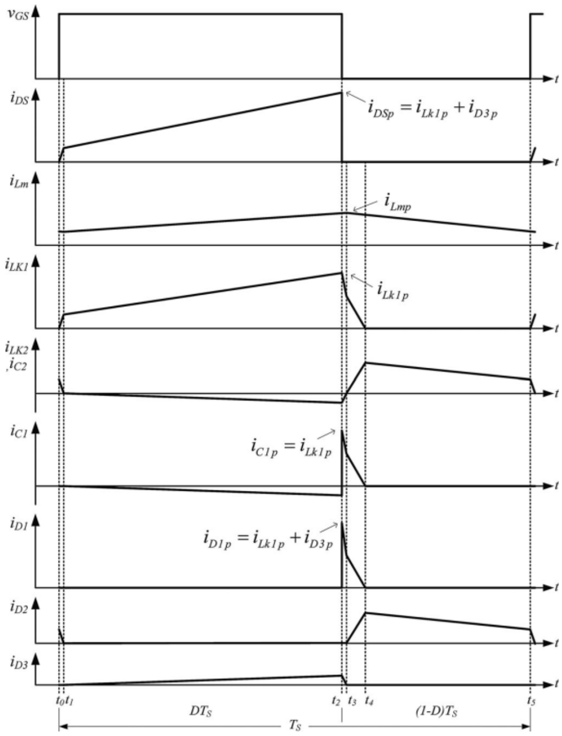

Fig 5 Waveforms of proposed converters at CCM operation

Mode 5 [t_4 , t_5]

During this interval, only magnetizing inductor L_m is constantly releasing its energy to C_2 .The current flow path is shown in Fig.4(d), in which only diode D_2 is conducting. The i_{Lm} is decreasing due to the magnetizing inductor energy flowing through the coupled inductor T1 to secondary winding N_2, and D_2 continues to charge capacitor C_2.The energy stored in capacitor C_3 is constantly discharged to the load R.[34] This mode ends when switch S_1 is turned ON at the beginning of the next switching period.

ISSN (Print) : 2320 – 3765
ISSN (Online): 2278 – 8875

International Journal of Advanced Research in Electrical, Electronics and Instrumentation Engineering

(An ISO 3297: 2007 Certified Organization)

Vol. 4, Issue 3, March 2015

III. STEADY-STATE ANALYSIS OF PROPOSED CONVERTERS

To simplify the steady-state analysis, only modes 2 and 4 are considered for CCM operation, and the leakage inductances on the secondary and primary sides are neglected. The following equations can be written from Fig. 4

$V_{Lm} = V_{in}$ 1

$V_{N2} = nV_{in}$ 2

During mode 4

$V_{Lm} = -V_{C1}$ 3

$V_{N2} = -V_{C2}$ 4

Applying a volt-second balance on the magnetizing inductor Lm yields,

$$\int_0^{DT_S} V_{IN}\,dt + \int_{DT_S}^{T_S} -V_{C1}\,dt = 0 \quad 5$$

$$\int_0^{DT_S} nV_{IN}\,dt + \int_{DT_S}^{T_S} -V_{12}\,dt = 0 \quad 6$$

From which the voltage across capacitors C_1 and C_2 are obtained as follows:

$$V_{C1} = \frac{D}{1-D} V_{IN} \quad 7$$

$$V_{C2} = \frac{nD}{1-D} V_{IN} \quad 8$$

During mode 2 the output voltage $V_O = V_{in} + V_{N2} + V_{C2} + V_{C1}$ becomes

$$V_O = V_{IN} + nV_{IN} + \frac{nD}{1-D} V_{IN} + \frac{D}{1-D} V_{IN} \quad 9$$

The DC voltage gain M_{CCM} can be found as follows

$$M_{CCM} = \frac{V_{OUT}}{V_{IN}} = \frac{1+n}{1-D} \quad 10$$

The voltage stresses on S_1 and D_1~ D_3 are given as

$$V_{DS} = V_{D1} = \frac{V_{IN}}{1-D} \quad 11$$

$$V_{D2} = \frac{nV_{IN}}{1-D} \quad 12$$

$$V_{D3} = \frac{(1+n)V_{IN}}{1-D} \quad 13$$

IV. EXPERIMENTAL RESULTS

A 100 W prototype sample is presented to verify the practicability of the proposed converter. The electrical specifications are V_{in}= 15 V, V_O= 200 V, f= 50 kHz, and full-load resistance R = 400 O. The major components required are C_S=47 µF and C3 = 220 µF. [35]Since assign turns ratio n = 5, the duty ratio D is derived as 55%. The following figures shows the PV output voltage, power output from converter , voltage and current waveforms, which are measured from active switch S and the current waveforms of C_1, C_2 and L_m..

ISSN (Print) : 2320 – 3765
ISSN (Online): 2278 – 8875

International Journal of Advanced Research in Electrical, Electronics and Instrumentation Engineering

(An ISO 3297: 2007 Certified Organization)

Vol. 4, Issue 3, March 2015

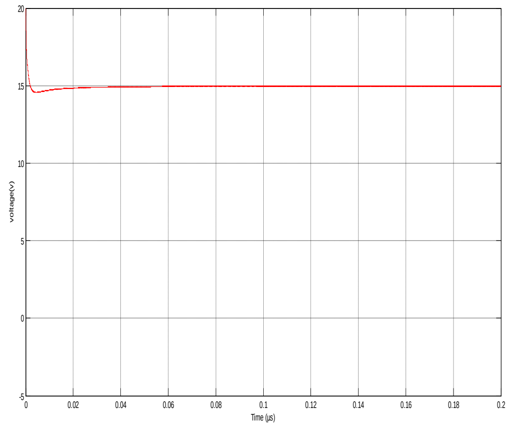

Fig 6 PV output voltage

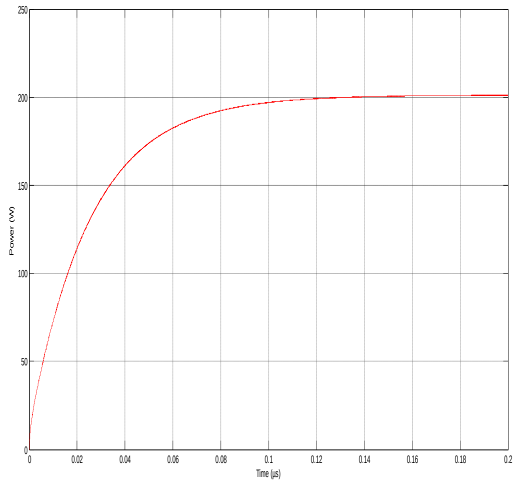

Fig 7 output power of boost converter

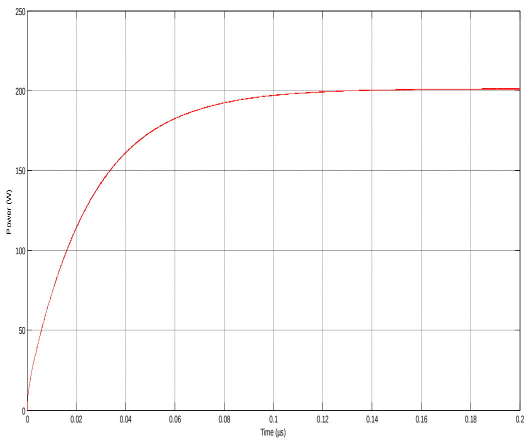

Fig 8 output power of boost converter

ISSN (Print) : 2320 – 3765
ISSN (Online): 2278 – 8875

International Journal of Advanced Research in Electrical, Electronics and Instrumentation Engineering

(An ISO 3297: 2007 Certified Organization)

Vol. 4, Issue 3, March 2015

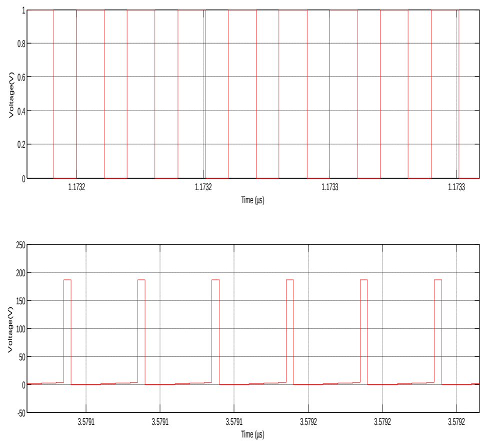

Fig 9 Gate voltage and voltage across switch

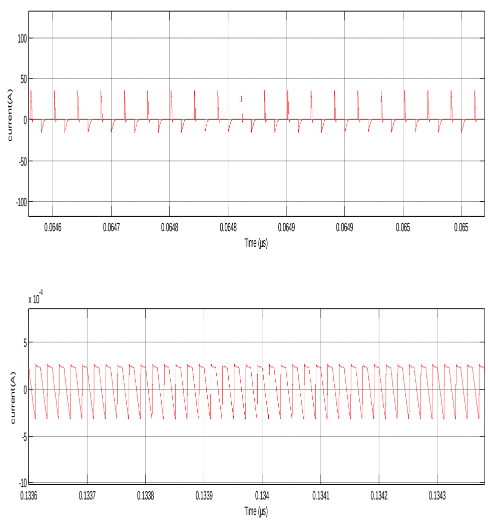

Fig 10 Current through C_1 and C_2

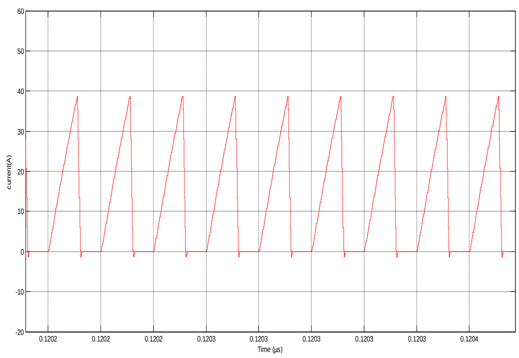

Fig..4.9 Current through L_m

ISSN (Print) : 2320 – 3765
ISSN (Online): 2278 – 8875

International Journal of Advanced Research in Electrical, Electronics and Instrumentation Engineering

(An ISO 3297: 2007 Certified Organization)

Vol. 4, Issue 3, March 2015

V. CONCLUSION

Since the energy of the coupled inductor's leakage inductor has been recycled, the voltage stress across the active switch S is constrained, which means low ON-state resistance $R_{DS(ON)}$ can be selected. Thus, improvements to the efficiency of the proposed converter have been achieved. The switching signal action is performed well by the floating switch during system operation; on the other hand, the residential energy is effectively eliminated during the non-operating condition, which improves safety to system technicians. From the prototype converter, the turns ratio n = 5 and the duty ratio D is 55%; thus, without extreme duty ratios and turns ratios, the proposed converter achieves high step-up voltage gain, of up to 13 times the level of input voltage.

REFERENCES

1. T.Shimizu,K.Wada and N.Nakamura, "Flyback-type single-phase utility interactive inverter with power pulsation decoupling on the dc input for an ac photovoltaic module system," IEEE Trans. Power Electron., vol. 21, no. 5, pp. 1264–1272, Jan. 2006.
2. C. Rodriguez and G. A. J. Amaratunga, "Long-lifetime power inverter for photovoltaic ac modules," IEEE Trans. Ind. Electron., vol. 55, no. 7, pp. 2593–2601, Jul. 2008.
3. Subha Palaneeswari M., Abraham Sam Rajan P.M., Silambanan S., Jothimalar, "Blood lead in end-stage renal disease (ESRD) patients who were on maintainence haemodialysis", Journal of Clinical and Diagnostic Research, ISSN : 0973 - 709X, 6(10) (2012) pp.1633-1635.
4. Sharmila S., Rebecca L.J., Saduzzaman M., "Effect of plant extracts on the treatment of paint industry effluent", International Journal of Pharma and Bio Sciences, ISSN : 0975-6299, 4(3) (2013) pp.B678-B686.
5. Saduzaman M., Sharmila S., Jeyanthi Rebecca L., 'Efficacy of leaf extract of Moringa oleifera in treating domestic effluent", Journal of Chemical and Pharmaceutical Research, ISSN : 0975 – 7384, 5(2) (2013) pp.139-143.
6. S. B. Kjaer, J. K. Pedersen, and F. Blaabjerg, "A review of single-phase grid-connected inverters for photovoltaic modules," IEEE Trans. Ind. Appl., vol. 41, no. 5, pp. 1292–1306, Sep./Oct. 2005.
7. J. J. Bzura, "The ac module: An overview and update on self-contained modular PV systems," in Proc. IEEE Power Eng. Soc. Gen. Meeting, Jul. 2010, pp. 1–3.
8. B. Jablonska, A. L. Kooijman-van Dijk, H. F. Kaan, M. van Leeuwen, G. T. M. de Boer, and H. H. C. de Moor, "PV-PRIV´E project at ECN, five years of experience with small-scale ac module PV systems," in Proc.20th Eur. Photovoltaic Solar Energy Conf., Barcelona, Spain, Jun. 2005,pp. 2728–2731.
9. Jeyanthi Rebecca L., Dhanalakshmi V., Sharmila S., "Effect of the extract of Ulva sp on pathogenic microorganisms", Journal of Chemical and Pharmaceutical Research, ISSN : 0975 – 7384 , 4(11) (2012) pp.4875-4878.
10. Sharmila D., Saravanan S., "Efficacy of lead on germination growth and morphological studies of Horse Gram (Dolichos biflorus Linn)", Journal of Chemical and Pharmaceutical Research, ISSN : 0975 – 7384 , 4(11) (2012) pp.4894-4896.
11. T. Umeno, K. Takahashi, F. Ueno, T. Inoue, and I. Oota, "A new approach to lowripple-noise switching converters on the basis of switched-capacitor converters," in Proc. IEEE Int. Symp. Circuits Syst., Jun. 1991, pp. 1077–1080.
12. B. Axelrod, Y. Berkovich, and A. Ioinovici, "Switched-capacitor/ switched-inductor structures for getting transformerless hybrid dc–dc PWM converters," IEEE Trans. Circuits Syst. I, Reg. Papers, vol. 55, no. 2, pp. 687–696, Mar. 2008.
13. B. Axelrod, Y. Berkovich, and A. Ioinovici, "Transformerless dc–dc converters with a very high dc line-to-load voltage ratio," in Proc. IEEE Int. Symp. Circuits Syst. (ISCAS), 2003, vol. 3, pp. 435–438.
14. S.Dwari and L. Parsa, "An efficient high-step-up interleaved dc–dc converter with a commonactive clamp," IEEE Trans.Power Electron., vol. 26, no. 1, pp. 66–78, Jan. 2011.
15. C. Restrepo, J. Calvente, A. Cid, A. El Aroudi, and R. Giral, "A noninverting buck-boost dc–dc switching converter with high efficiency and wide bandwidth," IEEE Trans. Power Electron., vol. 26, no. 9, pp. 2490–2503, Sep. 2011.
16. K. B. Park, G.W.Moon, andM. J. Youn, "Nonisolated high step-up boost converter integrated with sepic converter," IEEE Trans. Power Electron.,vol. 25, no. 9, pp. 2266–2275, Sep. 2010.
17. L. S. Yang, T. J. Liang, and J. F. Chen, "Transformerless dc–dc converters with high step-up voltage gain," IEEE Trans. Ind. Electron., vol. 56, no. 8,pp. 3144–3152, Aug. 2009.
18. N. Pogaku, M. Prodanovic, and T. C. Green, "Modeling, analysis and testing of autonomous operation of an inverter-based microgrid," IEEE Trans. Power Electron., vol. 22, no. 2, pp. 613–625, Mar. 2007.
19. Lingeswaran, K., "Microcontroller-based MPPT control for standalone PV system with sepic converter", Middle - East Journal of Scientific Research, v-20, i-8, pp:945-950, 2014.
20. Thamarai, P., Karthik, B., Kumaran, E.B., "Optimizing 2:1 MUX for low power design using adiabatic logic", Middle - East Journal of Scientific Research, v-20, i-10, pp:1322-1326, 2014.
21. Jayalakshmi, V., "Wireless sensor network for performance monitoring of electrical machine", Middle - East Journal of Scientific Research, v-20, i-8, pp:996-999, 2014.
22. Prasad, K.S., "A design towards smart batteries", Middle - East Journal of Scientific Research, v-20, i-10, pp:1318-1321, 2014.
23. Vijayaragavan, S.P., Karthik, B., Kiran Kumar, T.V.U., "Privacy conscious screening framework for frequently moving objects", Middle - East Journal of Scientific Research, v-20, i-8, pp:1000-1005, 2014.